Available online at www.sciencedirect.com

ScienceDirect

Procedia Engineering 00 (2011) 000–000

Procedia Engineering

www.elsevier.com/locate/procedia

11th International Conference on the Mechanical Behavior of Materials

Dynamic fracture of piezoelectric solid with defects

R. Mueller[a], D. Gross[b], T. Rangelov[c], P. Dineva[d]*

[a]*Chair of Applied Mechanics, Department of Mechanical and Process Engineering, Technical University Kaiserslautern, Kaiserslautern 67663, Germany*

[b]*Division of Solid Mechanics, Darmstadt University of Technology, Darmstadt 64289, Germany*

[c] *Institute of Mathematics and Informatics Bulgarian Academy of Sciences, Sofia 1113, Bulgaria*

[d] *Institute of Mechanics Bulgarian Academy of Sciences, Sofia 1113, Bulgaria*

Abstract

The main aim of this study is to propose, develop, validate and apply in intensive simulations an efficient non-hypersingular traction boundary integral equation method (BIEM) for solution of anti-plane dynamic fracture problems for piezoelectric solids with cracks or/and holes. The modelling approach is in the frame of continuum mechanics, wave propagation theory and linear fracture mechanics. The simulations reveal the sensitivity of stress concentration factor (SCF) and stress intensity factor (SIF) to coupled character of the electromechanical continuum, to type and characteristics of the dynamic load, to type of material, to the geometry of the solid and mutual defects' configuration and to defects interaction.

Keyword: piezoelectric solid, anti-plane cracks and holes, SCF/SIF, BIEM.

1. Introduction

Piezoelectric materials (PEM) are extensively applied in many modern technological fields due to their coupled electro-mechanical nature. At the same time their brittleness makes them sensitive against defects like cracks, holes or other type of imperfections. The understanding of the fracture process of PEM can provide useful information to improve the design of the electromechanical devices or to predict their lifetime. The present work is an effort in this direction.

The commonly used computational tools for evaluation of local generalized stress concentrations near defects like cracks and holes are wave function expansion method [1], matched asymptotic expansion [2], integral transform and singular integral equation method [3-5], finite element method [6], meshless methods [7], multi-domain [8], dual [9], hypersingular [10] and non-hypersingular [11,12] boundary

integral equation (BIE) techniques. The literature review shows that more of the obtained results are for unbounded solids with simple scenario and there exist few results for dynamic (time-harmonic) anti-plane fracture problems in finite piezoelectric solids.

The main aim of this study is to propose, develop, validate and use in simulations an efficient non-hypersingular traction BIEM and apply it for solution of anti-plane dynamic fracture problems for piezoelectric finite solids with cracks or/and holes.

The paper is organized as follows: The problem formulation via traction BIEs along external solid's boundary and defects' boundaries is given in Section 2. Validation and numerical results for different examples is presented in Section 3, followed by a discussion in Section 4.

2. Problem statement and its BIEM formulation

2.1. Problem statement

Consider finite linear piezoelectric transversely isotropic solid $G \subset R^2$ with boundary S in a Cartesian coordinate system $Ox_1x_2x_3$ and assume the material symmetry axis and poling axis are along Ox_3 axis. The solid is subjected to time-harmonic electro-mechanical load with a prescribed frequency ω. The analysis is carried out for anti-plane case according to plane $x_3 = 0$ and the nonzero field quantities are the displacement u_3, stresses σ_{13}, σ_{23}, electrical displacements D_1, D_2, electrical field components E_1, E_2, and electric potential Φ, all depending on x_1, x_2. The material characteristics are c_{44}, e_{15}, ε_{11}. Due to time-harmonic behaviour of all field quantities with frequency ω, the common multiplier $e^{i\omega t}$ is suppressed in the following.

The solid contains multiple defects like N^{cr} finite cracks Γ_m^{cr}, $m = 1,2,...N^{cr}$ with a half-length c_m and N^h circular holes H_k, $k = 1,2,...$ N^h of radius c_k and centre C_k, $\partial H_k = \Gamma_k^h$. Denote $\Gamma^{cr} = \bigcup_{m=1}^{N^{cr}} \Gamma_m^{cr}$, $\Gamma^h = \bigcup_{k=1}^{N^h} \Gamma_k^h$, and $\Gamma = \Gamma^{cr} \bigcup \Gamma^h$ and let us assume that all defects do not intersect each other, i.e. $\Gamma^{cr} \bigcap \Gamma^h = \varnothing$.

The mechanical and electrical balance equation in absence of body forces and electric charges can be written in a compact form via generalized filed variables u_K, σ_{iJ}, ρ_{JK} as

$$\sigma_{iJ,i} + \rho_{JK}\omega^2 u_K = 0 \qquad (1)$$

Where: $\rho_{JK} = \begin{cases} \rho, & J = K = 3 \\ 0, & J = 4 \quad or \quad K = 4 \end{cases}$; $u_K = \begin{pmatrix} u_3 \\ \Phi \end{pmatrix}$; $\sigma_{iJ} = \begin{pmatrix} \sigma_{13} \\ \sigma_{23} \\ D_1 \\ D_2 \end{pmatrix}$; ρ is density, subscript commas denote partial differentiation and the summation convention over repeated indices is applied. The boundary conditions on the outer boundary S is a prescribed displacement $u_J(\mathbf{x}) = \bar{u}_J(\mathbf{x})$, $\mathbf{x} \in S_u$ or/and traction $t_J(\mathbf{x}) = \bar{t}_J(\mathbf{x})$, $J = 3,4$ $\mathbf{x} \in S_t$, where $S = S_u \bigcup S_t$. Along the electrically impermeable defects traction free boundary conditions are assumed $t_J(\mathbf{x}) = 0$, $\mathbf{x} \in \Gamma$.

2.2. BIEM formulation

The equivalent formulation of the defined above BVP is derived via a system of non-hypersingular traction BIEs (2), (3) on the defects line Γ and on the external boundary S of the piezoelectric solid G following the approach proposed in Zhang and Gross [13] for elastic isotropic case and extended by the authors for piezoelectric case in [11,12].

$$\frac{1}{2}t_J^0(\mathbf{x}) = C_{iJKl}n_i\int_S[(\sigma^*_{\eta PK}(\mathbf{x},\mathbf{y})u^0_{P,\eta}(\mathbf{y}) - \rho_{QP}\omega^2 u^*_{QK}(\mathbf{x},\mathbf{y})u^0_P(\mathbf{y}))\delta_{\lambda l} - \sigma^*_{lPK}(\mathbf{x},\mathbf{y})u^0_{P,l}(\mathbf{y})]n_\lambda dS \qquad (2)$$
$$- C_{iJKl}n_i\int_S u^*_{PK,l}(\mathbf{x},\mathbf{y})t^0_P(\mathbf{y})dS, \text{ for } \mathbf{x}\in S$$

$$t_J(\mathbf{x}) = C_{iJKl}n_i\sum_{m=1}^{N^{cr}}\int_{\Gamma^{cr}_m}[(\sigma^*_{\eta PK}(\mathbf{x},\mathbf{y})\Delta u^{c,m}_{P,\eta}(\mathbf{y}) - \rho_{QP}\omega^2 u^*_{QK}(\mathbf{x},\mathbf{y})\Delta u^{c,m}_P(\mathbf{y}))\delta_{\lambda l} - \sigma^*_{lPK}(\mathbf{x},\mathbf{y})\Delta u^{c,m}_{P,l}(\mathbf{y})]n^m_\lambda d\Gamma^{cr}_m$$
$$+C_{iJKl}n_i\sum_{k=1}^{N^h}\int_{\Gamma^h_k}[(\sigma^*_{\eta PK}(\mathbf{x},\mathbf{y})u^{c,k}_{P,\eta}(\mathbf{y}) - \rho_{QP}\omega^2 u^*_{QK}(\mathbf{x},\mathbf{y})u^{c,k}_P(\mathbf{y}))\delta_{\lambda l} - \sigma^*_{lPK}(\mathbf{x},\mathbf{y})u^{c,k}_{P,l}(\mathbf{y})]n^k_\lambda d\Gamma^h_k \qquad (3)$$
$$-C_{iJKl}n_i\sum_{k=1}^{N^h}\int_{\Gamma^h_k}u^*_{PK,l}(\mathbf{x},\mathbf{y})t^{c,k}_P(\mathbf{y})d\Gamma^h_k + C_{iJKl}n_i\int_S[(\sigma^*_{\eta PK}(\mathbf{x},\mathbf{y})u^c_{P,\eta}(\mathbf{y}) - \rho_{QP}\omega^2 u^*_{QK}(\mathbf{x},\mathbf{y})u^c_P(\mathbf{y}))\delta_{\lambda l}$$
$$-\sigma^*_{lPK}(\mathbf{x},\mathbf{y})u^c_{P,l}(\mathbf{y})]n_\lambda dS - C_{iJKl}n_i\int_S u^*_{PK,l}(\mathbf{x},\mathbf{y})t^c_P(\mathbf{y})dS, \ \mathbf{x}\in S\cup\Gamma$$

here: $t_J = \begin{cases} -t^c_J/2 & on \quad S\cup\Gamma^h \\ -t^0_J & on \quad \Gamma^{cr} \end{cases}$; Δu^c_J is the generalized crack opening displacement; n^m_i, n^k_i is the outward normal vector at the observation point along the m^{th} crack and k^{th} hole; $\mathbf{x}$ and $\mathbf{y}$ is the source and observation points; u^*_{QK}, $\sigma^*_{iJM} = C_{iJKl}u^*_{KM,l}$ are the fundamental solution of Eq. (1) and its stress, derived and discussed in [11,12]; $C_{i33l} = \begin{cases} c_{44}, & i=l \\ 0, & i\neq l \end{cases}$, $C_{i34l} = \begin{cases} e_{15}, & i=l \\ 0, & i\neq l \end{cases}$, $C_{i44l} = \begin{cases} -\varepsilon_{11}, & i=l \\ 0, & i\neq l \end{cases}$; u^0_J, t^0_J are the variable fields due to the external load on the boundary S of the defect free body, while u^c_J, t^c_J are variable field induced by the load $t^c_J = -t^0_J$ on the defects boundary Γ with zero boundary conditions on the external boundary S, see [12]. Equations (2), (3) are integro-differential equations for the unknowns u^0_J, t^0_J and Δu^c_J, u^c_J, t^c_J resp. After discretization by quadratic boundary elements and special crack-tip elements near the crack-tips in order to model adequately the asymptotic behaviour of displacement as $\sqrt{r}$ and stress as $1/\sqrt{r}$ (r is the distance to the crack-tip), an algebraic system of equations for the unknowns is obtained and solved. The singular integrals converge in CPV sense, if the smoothness requirements in the approximation are fulfilled. The disadvantages of the standard quadratic approximation concerning the smoothness in all irregular points like crack-tips, corner points and odd nodes of the mesh is overcome by the usage of shifted point method, presented in details in [14]. The most essential quantities that characterize the mechanical and electric field concentrations are SIFs and SCFs. The stress intensity factors SIFs are obtained directly from the traction nodal values ahead of the

crack-tip: mechanical $\text{SIF-III} = \lim_{x_1 \to c} t_3 \sqrt{2\pi(x_1 \mp c)}$ and electrical $\text{SIF-IV} = \lim_{x_1 \to c} t_4 \sqrt{2\pi(x_1 \mp c)}$. They are normalized by the maximum amplitude of the traction τ_0 of the incident wave, where $\tau_0 = i\omega\sqrt{\rho\left(c_{44} + \frac{e_{15}^2}{\varepsilon_{11}}\right)}$. The SCFs (mechanical SCF-M and electrical SCF-E) are defined as the ratio of the stress and electric field along the circumference to the maximal amplitude of the incident stress at the same point. Knowing solution of the algebraic system, the displacement and traction in each one point of the considered solid can be obtained by using the representation formulae.

3. Numerical illustration of validation and simulation study

In order to validate the proposed BIEM three benchmark examples for a finite quadratic plate with size $b >> 10c$ and with a circular hole-horizontal crack system (Fig.1a) subjected to incident SH wave with normalized frequency $\Omega = c\omega\sqrt{\rho c_{44}^{-1}}$ are solved in the following cases: *(i)* the distance between both defects is $h = 5c$ and comparison with results in [15] for a single hole in a plane under SH-wave propagating in positive Ox_1 direction; *(ii)* $h = c$ and comparison with results in [16] for a hole-horizontal crack system in a plane of two different PZT-4 with $m = (e_{15}^2 / c_{44}\varepsilon_{11})$ under normal to the crack SH-wave ; *(iii)* $h = 5c$ and comparison with results in [3] for a single crack in a plane under mechanical load with amplitude τ and electrical one with amplitude $s\tau(\varepsilon_{11} / e_{15})$.

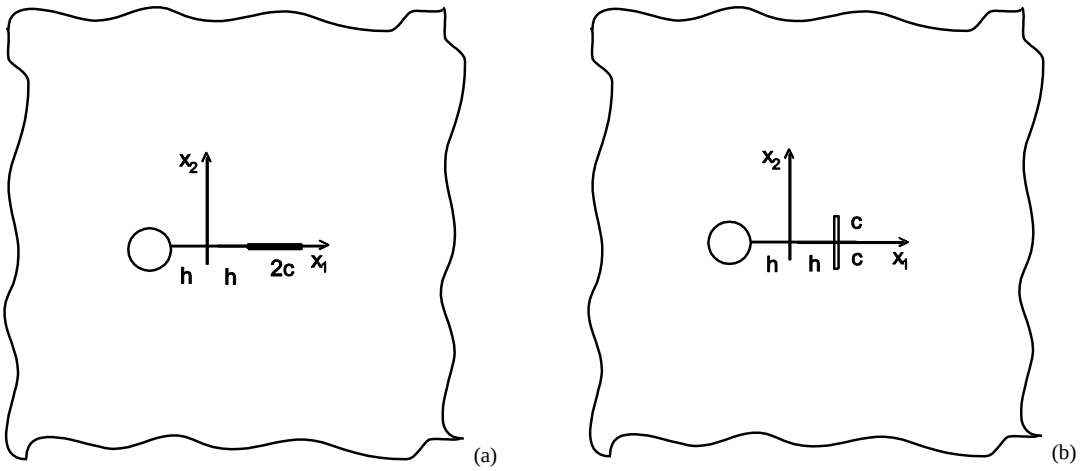

Fig. 1 Piezoelectric solid with a hole-crack system: (a) hole-horizontal crack; (b) hole-vertical crack.

As far as the existing in the literature solutions are only for unbounded domains, we test our procedure by representing the infinite domain as a truncated square with a size $b >> 10c$. At distance between both defects $h = 5c$, the hole-crack interaction is very weak and the solution of the boundary-value problem for the system hole-crack recovers solutions for the single hole and single crack. Figures 2, 3 present all *(i)-(iii)* cases and demonstrate that the proposed numerical scheme works with high accuracy and convergence in the considered frequency interval. Fig. 4a, b present SCFs at observer p. $A\ (-h, 0.0)$ of a

hole-crack system in finite piezoelectric plate vs frequency of incident SH-wave with $\theta = 0$ at different distances between hole and crack (see Fig. 1b, c) $h = 0.25c$; $0.5c$ and at different configurations of both defects- hole-horizontal crack and hole-vertical crack. All simulations done show that dynamic stress concentration fields near the defects expressed by the SCFs along the hole's boundary and SIFs near the crack-tips are influenced significantly by the hole-crack configuration, its geometry, type and characteristics of the applied load and phenomena like defect-defect and wave-defect interactions.

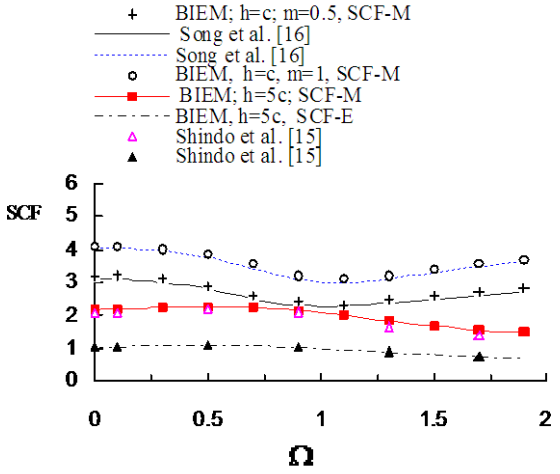

Fig. 2 SCFs at p. A $(-h, 0.0)$ versus Ω for a hole-horizontal crack system (Fig.1a) at $h = 5c$ and $h = c$ under time-harmonic load.

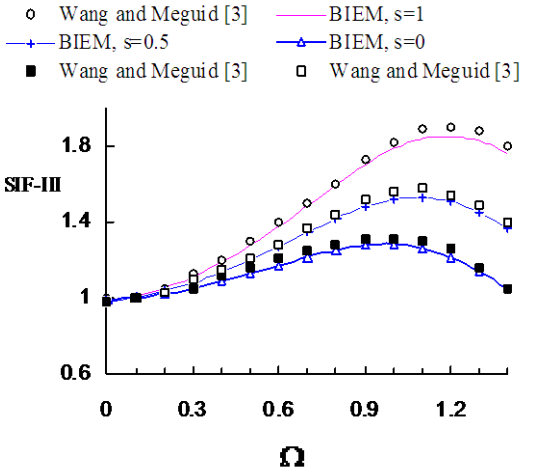

Fig. 3 SIF-III at p. A $(+h, 0.0)$ versus Ω for a hole-horizontal crack system (Fig.1a) at $h = 5c$ under time-harmonic load.

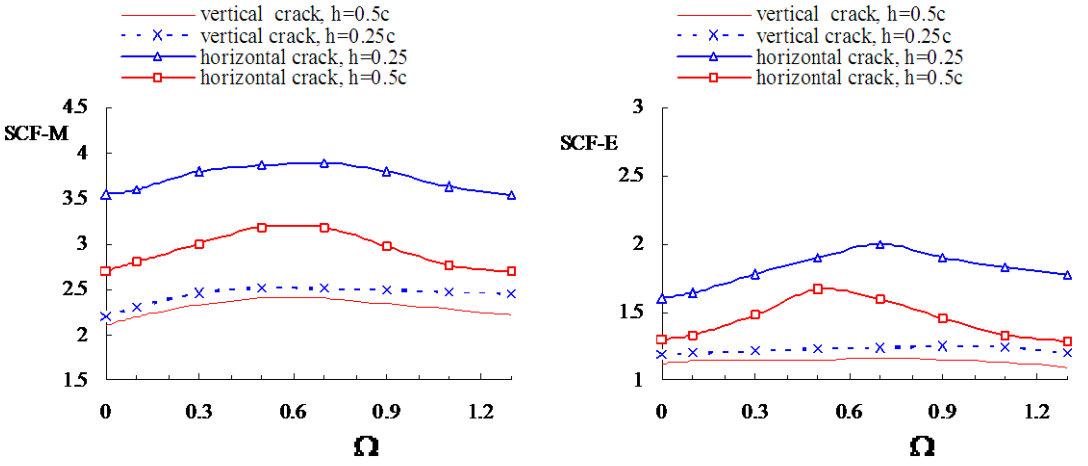

Fig. 4a, b: SCFs at p. $A\ (-h, 0.0)$ for a hole-horizontal /vertical crack system (Fig.1a, b) versus Ω of time-harmonic load: (a) SCF-M; (b) SCF-E.

4. Conclusion

The numerical results reveal the sensitivity of the dynamic stress and electric field concentrations in a piezoelectric solid with different type of defects to the geometry of the considered scenario, to the coupled character of the electromechanical continuum, to the type and characteristics of the dynamic load, to the defects existence and their interaction. The application of the near-field solutions is in computational fracture mechanics of PEM, while the knowledge for the wave far-field solutions can be used for non-destructive evaluation of multifunctional materials and the smart structures based on them.

Acknowledgements

The authors acknowledge the support of the Deutsche Forschungsgemeinschaft under the grant number: 436BUL 113/150/0-1 and the support of the Bulgarian National Science Fund under the grant number: DID 02/15.

References

[1] Shindo Y, Minamida K, Narita F. Antiplane shear wave scattering from two curved interface cracks between a piezoelectric fiber and an elastic matrix. *Smart Materials and Structures* 2002; 11(4):534-540.

[2] Kulikov AA, Nazarov SA. Cracks in piezoelectric and electricconducting bodies. *Siberian Journal of Industrial Mathematics* 2005; 8:70-87.

[3] Wang XD, Meguid SA. Modelling and analysis of the dynamic behaviour of piezoelectric materials containing interfacing cracks. *Mechanics of Materials* 2000; 32: 723–737.

[4] Shindo Y, Ozawa E. Dynamic analysis of a cracked piezoelectric material. In: Hsieh RKT, editor. *Mechanical Modelling of New Electromagnetic materials*, Amsterdam: Elsevier; 1990, p.297-304.

[5] Narita F, Shindo Y. Dynamic anti-plane shear of a cracked piezoelectric ceramics. *Theoretical and Applied Mechanics* 1998; 29: 169– 180.

[6] Kuna M. Finite element analysis of cracks in piezoelectric structures: a survey. *Archive of Applied Mechanics* 2006; 76: 725-745.

[7] Guo XH, Fang DN. Analysis of Piezoelectric Fracture under Combined Mechanical and Electrical Loading based on Meshless Method. *Key Engineering Materials* 2004; 261-263: 543-548.

[8] Davì G, Milazzo A. Multidomain boundary integral formulation for piezoelectric materials fracture mechanics. *International Journal of Solids and Structures* 2001; 38: 7065-7078.

[9] Pan E. A BEM analysis of fracture mechanics in 2D anisotropic piezoelectric solids. *EABE* 1999; 23(1): 67-76.

[10] Gross D, Rangelov T, Dineva P. 2D wave scattering by a crack in a piezoelectric plane using traction BIEM. *Journal Structural Integrity & Durability* 2005; 1(1): 35-47.

[11] Dineva P., Gross D., Müller R., Rangelov T. Dynamic stress and electric field concentration in a functionally graded piezoelectric solid with a circular hole. *ZAMM* 2011; 91(2): 110-124.

[12] Dineva P, Gross D, Müller R, Rangelov T. BIEM analysis of dynamically loaded anti-plane cracks in graded piezoelectric finite solids. *International Journal of Solids and Structures* 2010; 47(22-23: 3150-3165.

[13] Zhang Ch, Gross D. *On wave propagation in elastic solids with cracks.* Southampton: Comp. Mech. Publ.; 1998.

[14] Rangelov T., Dineva P., Gross D. A hypersingular traction boundary integral equation method for stress intensity factor computation in a finite cracked body. *EABE* 2003; 27(1): 9-21.

[15] Shindo Y, Moribayashi H, Narita. F. Scattering of antiplane shear waves by a circular piezoelectric inclusion embedded in a piezoelectric medium subjected to a steady-state electrical load. *ZAMM* 2002; 82:43-49.

[16] Song T., Li H, Dong J. Dynamic anti-plane behaviour of the interaction between a crack and a circular cavity in a piezoelectric medium. *Key Engineering Materials* 2006; 324, 325: 29-32.